A SEARCH FOR VERY HIGH ENERGY NEUTRINOS WITH THE BAIKAL NEUTRINO TELESCOPE

V.BALKANOV, L.BEZRUKOV, I.DANILCHENKO, Zh.-A.DZHILKIBAEV, G.DOMOGATSKY, A.DOROSHENKO, O.GAPONENKO, A.KLABUKOV, S.KLIMUSHIN, A.KOSHECHKIN, Vy.KUZNETZOV, B.LUBSANDORZHIEV, V.NETIKOV, A.PANFILOV, E.PLISKOVSKY, P.POKHIL, V.POLESHUK, R.VASILJEV, V.ZHUKOV

Institute for Nuclear Research, 60-th October Anniversary prospect, Moscow 117312, Russia

E-mail: djilkib@pcbai10.inr.ruhep.ru

N.BUDNEV, A.CHENSKY, O.GRESS, J.LJAUDENSKAITE, R.MIRGAZOV, L.PAN'KOV, Yu.PARFENOV, A.PAVLOV, V.RUBZOV, Yu.SEMINEI, B.TARASHANSKY

Irkutsk State University, Irkutsk, Russia

L.KUZMICHEV, N.MOSEIKO, E.OSIPOVA, E.POPOVA, V.PROSIN, I.YASHIN

Institute of Nuclear Physics, Moscow State University, Moscow, Russia

S.FIALKOVSKY, V.KULEPOV, M.MILENIN

Nizhni Novgorod State Technical University, Nizhni Novgorod , Russia

M.ROZANOV

St.Petersburg State Marine Technical University, St.Petersburg, Russia

A.KLIMOV

Kurchatov Institute, Moscow, Russia

I.BELOLAPTIKOV

Joint Institute for Nuclear Research, Dubna, Russia

Ch.SPIERING, O.STREICHER, T.THON, R.WISCHNEWSKI

DESY-Zeuthen, Zeuthen, Germany

and

D.KISS, G.TOTH

KFKI, Budapest, Hungary

ABSTRACT

We present the results of a search for high energy neutrinos with the Baikal underwater Cherenkov detector *NT-200*. An upper limit on the $(\nu_e + \tilde{\nu_e})$ diffuse flux of $E^2\Phi_\nu(E) < (1.3 \div 1.9) \cdot 10^{-6}\,\mathrm{cm}^{-2}\,\mathrm{s}^{-1}\,\mathrm{sr}^{-1}\,\mathrm{GeV}$ within a neutrino energy range $10^4 \div 10^7\,\mathrm{GeV}$ is obtained, assuming an E^{-2} behaviour of the neutrino spectrum and flavor ratio $(\nu_e + \tilde{\nu_e}) : (\nu_\mu + \tilde{\nu_\mu})$=1:2.

1. Introduction

The Baikal Neutrino Telescope is deployed in Lake Baikal, Siberia, 3.6 km from shore at a depth of 1.1 km. The optical properties of Lake Baikal deep water are

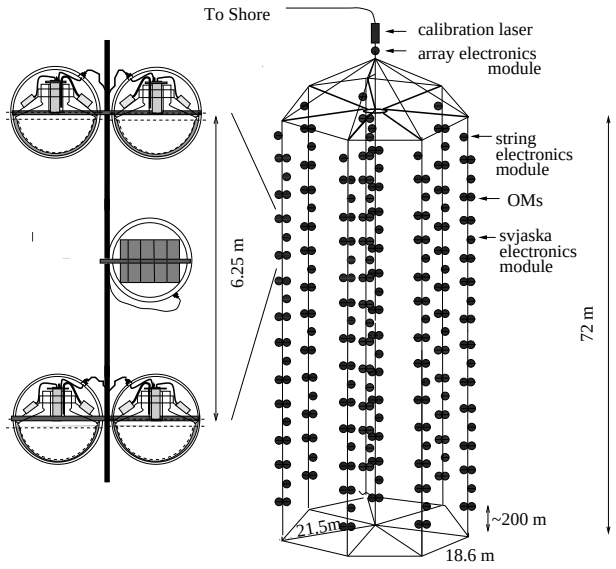

Figure 1: Schematic view of the Baikal neutrino telescope.

characterized by an absorption length of 20÷ 25 m, a scattering length of 20÷70 m and a strongly anisotropic scattering function $f(\theta)$ with mean cosine of scattering angle $\overline{\cos}(\theta)$=0.85÷0.95. *NT-200*, the medium-term goal of the collaboration [1)], was put into operation on April 6th, 1998 and consists of 192 optical modules (OMs). An umbrella-like frame (see Fig.1) carries 8 strings, each with 24 pairwise arranged OMs. Three underwater electrical cables and one optical cable connect the detector with the shore station.

The OMs are grouped in pairs along the strings. They contain 37-cm diameter *QUASAR* - photomultipliers (PMs) which have been developed specially for our project [2)]. The two PMs of a pair are switched in coincidence in order to suppress background from bioluminescence and PM noise. A pair defines a *channel*.

A *muon-trigger* is formed by the requirement of ≥4 *hits* (with *hit* referring to a channel) within 500 ns. For such events, amplitude and time of all fired channels are digitized and sent to shore. Full space-angular track reconstruction is possible for muon induced events with ≥6 hits at ≥3 strings (*off-line trigger* 6/3). A separate *monopole trigger* system searches for clusters of sequential hits in individual channels which are characteristic for the passage of slowly moving, bright objects like GUT monopoles.

Table 1 illustrates *NT-200* operation efficiency since April 1998 till February 2001. Shown are the data taking time T, the fraction T/T_{tot} of total detector operating time T_{tot} when data have been taken, the number of accumulated events N_{ev}, the number of events allowing full space-angular track reconstruction $N_{ev}(6/3)$, the average fraction of working channels N_{op}/N_{tot} as well as the data taking time T(>85%) with ≥85% channels in operation.

Table 1: *NT-200* - operation efficiency

Years	T (days)	T/T_{tot}	N_{ev} (10^6 events)	$N_{ev}(6/3)$ (10^6 events)	N_{op}/N_{tot}	T(>85%) (days)
98-99	234	73%	167	57	71%	8
99-00	236	75%	191	65	76%	61
00-01	245	79%	233	82	81%	120

Using the data accumulated during first 234 livetime days between April 1998 and February 1999, 35 neutrino induced upward muons have been reconstructed [3]. Although in a good agreement with MC expectation this number is by a factor 3 lower than predicted for the fully operational *NT-200*. The reason is that, due to unstable operation of electronics, in average only 50 - 70 channels have taken data during 1998. This is in contrast to 1999 and 2000 data taking where the stability had been improved. Ten events within a 30 degree half angle cone around nadir have been selected to set limits on the excess of the muon flux due to WIMP annihilation in the center of the Earth. Also a new limit on the flux of fast monopoles has been obtained [3].

Here we present preliminary results from a search for high energy neutrinos (E_ν >10 TeV) with *NT-200* obtained from the analysis of the entire 1998 data set.

2. A search for high energy neutrinos

The main goal of large underwater neutrino telescopes is the search for extraterrestrial high energy neutrinos. Detection volume and detection area of such detectors depend on the transparency of the medium (water or ice) and the power of the source of Cherenkov radiation (high energy shower or muon), and may significantly exceed the geometrical one.

2.1. Search strategy

The used search strategy for high energy neutrinos relies on the detection of the Cherenkov light emitted by the electro-magnetic and (or) hadronic particle cascades and high energy muons produced at the neutrino interaction vertex in a large volume around the neutrino telescope. Earlier, a similar strategy has been used by DUMAND [4], AMANDA [5] and BAIKAL [6] collaborations to obtain upper limits on the diffuse flux of high energy neutrinos with relatively small detectors (SPS, AMANDA-A and *NT-96*, respectively). Although the limits implied by these observations are at least one order of magnitude higher then the model independent upper limit derived from the energy density of the diffuse X- and gamma-radiation [8], these results illustrate the power of used search strategy.

Neutrinos produce showers through CC-interactions

$$\nu_l(\bar{\nu}_l) + N \xrightarrow{CC} l^-(l^+) + \text{hadrons}, \tag{1}$$

through NC-interactions

$$\nu_l(\bar{\nu}_l) + N \xrightarrow{NC} \nu_l(\bar{\nu}_l) + \text{hadrons}, \tag{2}$$

where $l = e$, μ or τ, and through resonance production [9,10,12)]

$$\bar{\nu_e} + e^- \to W^- \to \text{anything}, \tag{3}$$

with the resonant neutrino energy $E_0 = M_w^2/2m_e = 6.3 \cdot 10^6$ GeV and cross section $5.02 \cdot 10^{-31}\text{cm}^2$.

We select events with high multiplicity of hit channels N_{hit} corresponding to bright cascades. The volume considered for generation of cascades is essentially *below* the geometrical volume of *NT-200*. A cut is applied which accepts only time patterns corresponding to upward traveling light signals (see below). This cut rejects most events from brems-cascades produced by downward going muons since the majority of muons is close to the vertical; they would cross the detector and generate a downward time pattern. Only the fewer muons with large zenith angles may escape detection and illuminate the array by their proper Cherenkov radiation or via bright cascades from below the detector. These events then have to be rejected by a stringent multiplicity cut.

The used strategy is very effective for ν_e and ν_τ detection since the main fraction of neutrino energy would be transfered to electro-magnetic or/and hadronic cascades due to CC-interactions. It is less effective for ν_μ detection since the main part of neutrino energy would be escaped by energetic muon from detection volume. For ν_μ search preliminary result has been presented by the AMANDA experiment [7)].

2.2. Data

Within the 234 days of the detector livetime, $1.67 \cdot 10^8$ events with $N_{hit} \geq 4$ have been selected. For this analysis we used events with N_{hit} >10. The time difference between any two hit channels on the same string was required to obey the condition:

$$(t_i - t_j) > -10 \text{ ns}, \;\; (i < j), \tag{4}$$

where t_i, t_j are the arrival times at channels i, j and the numbering of channels rises from top to bottom along the string.

Since April 1998 till February 1999, *NT-200* operated in 3 main configurations with 77, 60 and 49 working channels, respectively. Data taking time T, the number of selected events N_{ev} which survive cut (4) and the maximum hit multiplicity N_{hit}^{max} of these events. are shown in Table 2.

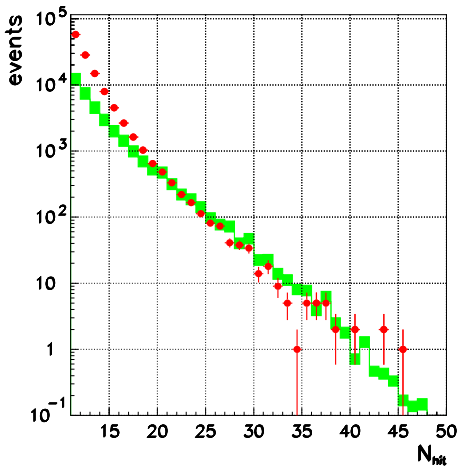

Figure 2: Distribution of hit channels multiplicity; dots - experiment, hatched boxes - expectation from brems and hadronic showers produced by atmospheric muons.

Table 2: *NT-200* configurations in 1998.

Configuration	N_{op}	T (days)	N_{ev}	N_{hit}^{max}	N_{thr}
1	77	57.9	63540	45	50
2	60	145.8	83319	37	39
3	49	30.9	8719	24	26

Fig.2 shows the hit multiplicity distribution of selected (dots) as well as the expected one from background high energy brems and hadronic showers produced by atmospheric muons (hatched boxes). The experimental distribution is consistent with the theoretical expectation for N_{hit} >18. For lower N_{hit} values the contribution of atmospheric muons close to horizon as well as low energy showers from e^+e^- pair production become important. The highest multiplicity of hit channels experimentally observed is $N_{hit}^{max} = 45$ (one event). No statistically significant excess over expectation from atmospheric muon induced showers has been observed for each of the 3 detector configurations. The detection efficiency of *NT-200* for events with $N_{hit} > N_{hit}^{max}$ had been analysed by applying several less stringent cuts. It was shown that the experimental N_{hit} distributions are consistent with expected ones from atmospheric muons.

Since no events with $N_{hit} > N_{hit}^{max}$ are found in our data we can derive upper limits on the flux of high energy neutrinos which would produce events with

$$N_{hit} > N_{thr}, \tag{5}$$

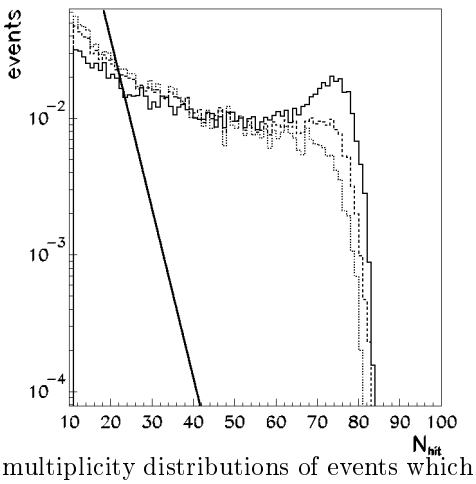

Figure 3: The normalized hit multiplicity distributions of events which would be produced by the ν_e fluxes and survive the selection criterion (4). Solid, dashed and dotted curves correspond to γ=1.5, 2, 2.5, respectively. Also shown is the normalized N_{hit} distribution of events from atmospheric muon induced showers (thick line).

where the chosen values of N_{thr} for the 3 detector configurations are given in Table 2.

2.3. MC-simulations

Given an isotropic diffuse high energy neutrino flux with power law energy spectrum with spectral index γ, the number of expected events during observation time T reads

$$N_\nu = \frac{A_\nu T}{4\pi} \int d\Omega \int dE V_{eff}(\Omega, E) \sum_k \int dE_\nu E_\nu^{-\gamma} N_A \rho_{H_2O} \frac{d\sigma_{\nu k}}{dE} \exp(-l(\Omega)/l_{tot}) \qquad (6)$$

where E_ν is the neutrino energy, E - the energy transferred to a shower, A_ν - normalization coefficient of neutrino flux and $V_{eff}(\Omega, E)$ - detection volume [a]. The index ν indicates neutrino types ($\nu = \nu_\mu, \tilde{\nu_\mu}, \nu_e, \tilde{\nu_e}$) and k indicates the summation over CC and NC interactions. N_A is the Avogadro number. Cross sections [11,12] $d\sigma_{\nu k}/dE$ correspond to processes (1) and (2). The neutrino absorption in the Earth has been taken into account with a suppression factor $\exp(-l(\Omega)/l_{tot})$, where $l(\Omega)$ is the neutrino path length through the Earth in direction Ω and $l_{tot}^{-1} = N_A\, \rho_{Earth}\, (\sigma_{CC} + \sigma_{NC})$ according to [11,12].

In Fig.3 we show the normalized predictions of N_{hit} distributions of events which survive cut (4) and would be induced by electron neutrino fluxes with γ=1.5, 2, 2.5. The normalized N_{hit} distribution of events from atmospheric muon induced showers, which has strongly steeper behaviour, is also presented.

[a] In a case of ν_μ CC- interaction in water the detector response to hadronic shower as well as to the high energy muon has been taken into account.

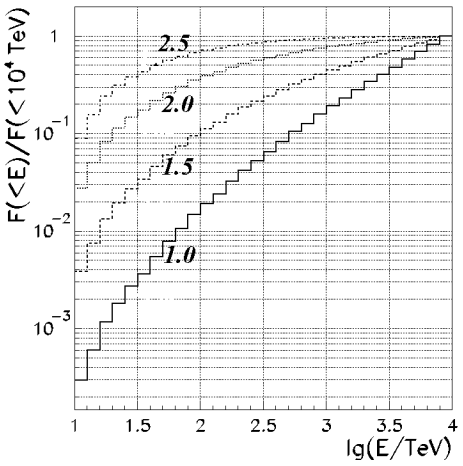

Figure 4: The fractions of expected events induced by diffuse ν_e fluxes with spectral indexes γ=1, 1.5, 2, 2.5 within energy range 10 TeV<E_ν <E.

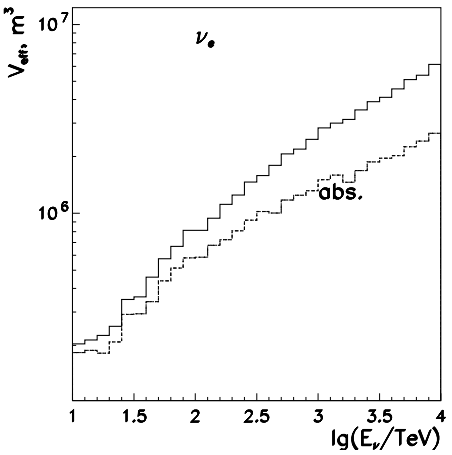

Figure 5: Detection volume of ν_e produced events which survive cuts (4)-(5) (upper curve). The detection volume folded with the neutrino absorption probability in the Earth (lower curve) is also shown.

The neutrino detection energy range of *NT-200* which contains, for instance, 90% of expected events, depends on the value of spectral index γ. Normalized energy distributions of expected events induced by electron neutrinos within energy range 10 TeV $\div$ E (E<10^4 TeV) and different γ are presented in Fig.4. Assuming γ =2 as typically expected for Fermi acceleration, 90% of expected events would be produced by neutrinos from the energy range 20 $\div$ 10^4 TeV with the mean energy around 200 TeV.

The detection volume for neutrino produced events which fulfill conditions (4)-(5) was calculated as a function of neutrino energy and zenith angle θ. The energy dependence of the detection volume for isotropic ν_e flux with γ =2 is shown in Fig.5. Also shown is the detection volume folded with the neutrino absorption probability

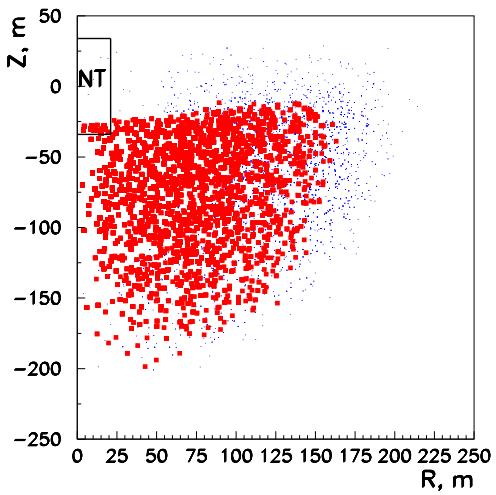

Figure 6: Coordinates of ν_e interaction vertex for events which fulfill conditions (4) (dots) and (4)-(5) (rectangles).

in the Earth. The value of V_{eff} rises from $2{\cdot}10^5$ m^3 for 10 TeV up to $6{\cdot}10^6$ m^3 for 10^4 TeV and significantly exceeds the geometrical volume $V_g \approx 10^5$ m^3 of *NT-200*. This is due to the low light scattering and the preserved light fronts from Cherenkov waves originating far outside the geometrical volume. Although the detection volume has been calculated without taking into account light scattering in the water, estimations show that a scattering with L_s=20 m and $\overline{\cos}(\theta)$=0.88 (conservative values for Lake Baikal water) would cause $\leq$30% decrease of V_{eff} for $E_\nu \leq 10^3$TeV.

Fig.6 illustrates the difference between V_{eff} and V_g. Shown here are the coordinates of neutrino interaction vertex for events which survive cuts (4) (dots) and (4)-(5) (rectangles).

2.4. The limits on the high energy neutrino fluxes

The shape of the neutrino spectrum was assumed to behave like E^{-2} and flavor ratio $(\nu_e + \tilde{\nu_e}) : (\nu_\mu + \tilde{\nu_\mu}) = 1 : 2$ due to photo-meson production of π^+ followed by the decay $\pi^+ \to \mu^+ + \nu_\mu \to e^+ + \nu_e + \bar{\nu_\mu} + \nu_\mu$ for extraterrestrial sources.

Comparing the expected number of events fulfilling (4)-(5) with the upper limit on the actual number of events, 2.4 for 90% C.L. [13] we obtain the upper limit on the diffuse $(\nu_e + \tilde{\nu_e})$ flux. The combined upper limit obtained with Baikal neutrino telescopes *NT-200* (234 days) and *NT-96* [6] (70 days) is:

$$\Phi_{(\nu_e+\tilde{\nu_e})} E^2 < (1.3 \div 1.9) \cdot 10^{-6} \mathrm{cm}^{-2}\mathrm{s}^{-1}\mathrm{sr}^{-1}\mathrm{GeV}, \qquad (7)$$

where the upper value refers to the conservative limit on light scattering in the Baikal water.

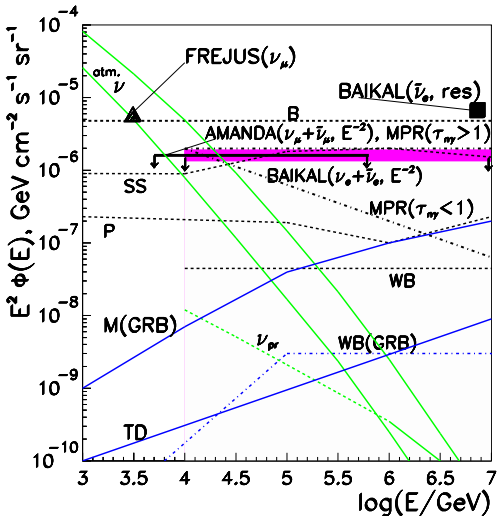

Figure 7: The upper limits on the diffuse neutrino fluxes, obtained by BAIKAL (this work: for E^{-2} flux as well as for a model independent $\tilde{\nu}_e$ flux at resonant energy $6.3{\cdot}10^6$GeV (rectangle)), AMANDA [7] and FREJUS [14] (triangle) experiments as well as the atmospheric conventional neutrino fluxes [15] from horizontal and vertical directions (upper and lower curves, respectively) and atmospheric prompt neutrino flux [16] (curve labeled ν_{pr}). The limits and predictions from different models of high energy neutrino sources are also shown. Curves labeled 'B', 'MPR' and 'WB' represent the model independent limit derived by Berezinsky [8] and the upper bounds derived by Mannheim et al. [20] as well as by Waxman and Bahcall [21]. Curves labeled as 'SS' and 'P' show predicted fluxes from quasar cores and blazar jets derived by Stecker and Salamon [18] and Protheroe [19] respectively. Curves labeled 'M(GRB)' and 'WB(GRB)' represent predicted fluxes from GRBs derived by Mannheim [22] and Waxman and Bahcall [23]. Curve labeled 'TD' - prediction for neutrino flux from topological defects due to specific top-down scenario BHS1 [24].

Fig.7 shows the upper limits on the isotropic diffuse high energy neutrino fluxes obtained by BAIKAL (this work), AMANDA [7] and FREJUS [14] (triangle) experiments as well as the atmospheric conventional neutrino fluxes [15] from horizontal and vertical directions (upper and lower curves, respectively) and atmospheric prompt neutrino flux [16] (curve labeled ν_{pr}). Also shown is the model independent upper limit on the diffuse high energy neutrino flux obtained by V.Berezinsky [8] (curve labeled 'B') with the energy density of the diffuse X- and gamma-radiation $\omega_x \leq 2{\cdot}10^{-6}$ eV cm^{-3} (as follows from EGRET data [17]), and predictions for diffuse neutrino fluxes from Stecker and Salamon model [18] (the sum of the quasar core and blazar jet contribution, curve labeled 'SS') and Protheroe model [19] (from equal contribution from pp and $p\gamma$ interactions in AGN jets, curve labeled 'P'). Curves labeled 'MPR' and 'WB' show the upper bounds obtained by Mannheim, Protheroe and Rachen [20] for optically thick ($\tau_{n\gamma} > 1$) and optically thin ($\tau_{n\gamma} < 1$) sources as well as the upper bound obtained by Waxman and Bahcall [21] for optically thin sources respectively. Curves labeled 'M(GRB)' and 'WB(GRB)' present the upper bounds for diffuse neutrino flux from GRBs derived by Mannheim [22] and Waxman and Bahcall [23]. Curve labeled 'TD' shows prediction for neutrino flux from topological defects due to specific top-down scenario BHS1 [24].

For the resonant process (3) the event number is given by:

$$N_{\bar{\nu_e}} = T \int d\Omega \int dE V_{eff}(\Omega, E) \int\limits_{(M_w - 2\Gamma_w)^2/2m_e}^{(M_w + 2\Gamma_w)^2/2m_e} dE_\nu \Phi_{\bar{\nu_e}}(E_\nu) \frac{10}{18} N_A \rho_{H_2O} \frac{d\sigma_{\bar{\nu_e}, e}}{dE} \qquad (8)$$

$$M_w = 80.22\text{GeV}, \ \ \Gamma_w = 2.08\text{GeV}.$$

Our combined 90% C.L. limit obtained with *NT-200* and *NT-96* [6] at the W - resonance energy is:

$$\frac{d\Phi_{\bar{\nu}}}{dE_{\bar{\nu}}} \leq (1.4 \div 1.9) \times 10^{-19} \text{cm}^{-2}\text{s}^{-1}\text{sr}^{-1}\text{GeV}^{-1}. \qquad (9)$$

and is also depicted in Fig.7 (rectangle).

3. Conclusion

The deep underwater neutrino telescope *NT-200* in Lake Baikal is taking data since April 1998. Due to the high water transparency and low light scattering, the detection volume of *NT-200* for high energy ν_e and ν_τ detection is several megatons and exceeds the geometrical volume by factor of about 50 for highest energies. This permits a search for diffuse neutrino fluxes from extraterrestrial sources on the level of theoretical predictions. The upper limits (7), (9) obtained for the diffuse E^{-2} $(\nu_e + \tilde{\nu_e})$ flux and the model independent $\tilde{\nu_e}$ flux at resonant energy $6.3{\cdot}10^6$GeV are the most stringent ones at present. We expect that the analysis of 3 years data taken with *NT-200* would allow us to reach a sensitivity of $\Phi_\nu E^2 \approx 6 \cdot 10^{-7} \text{cm}^{-2}\text{s}^{-1}\text{sr}^{-1}\text{GeV}$.

4. Acknowledgements

This work was supported by the Russian Ministry of Research (contract 102-11(00)-p), the German Ministry of Education and Research and the Russian Fund of Basic Research (grants 99-02-18373a, 01-02-31013 and 00-15-96794), and by the Russian Federal Program "Integration" (project no. 346).

5. References

1) I.A.Belolaptikov *et al.*, *Astropart. Phys.* **7** (1997) 263.
2) R.I.Bagduev *et al., Nucl. Instr. Meth.* **A420** (1999) 138.
3) V.A.Balkanov *et al.*, *Nucl. Phys. Proc. Suppl.* **91** (2001) 438.
4) J.W.Bolesta *et al.*, *Proc. 25-th ICRC* Durban–South Africa, **7** (1997) 29.
5) R.Porrata *et al.*, *Proc. 25-th ICRC* Durban–South Africa, **7** (1997) 9.
6) V.A.Balkanov *et al.*, *Astropart. Phys.* **14** (2000) 61.

7) E.Andres *et al.*, *Nucl. Phys. Proc. Suppl.* **91** (2001) 423.
8) V.S.Berezinsky *et al., Astrophysics of Cosmic Rays,* North Holland, Amsterdam (1990).
9) S.L.Glashow, *Phys. Rev.* **118** (1960) 316.
10) V.S.Berezinsky and A.Z.Gazizov, *JETP Lett.* **25** (1977) 254.
11) V.S.Berezinsky *et al., Sov. J. Nucl. Phys.* **43** (1986) 406.
12) R.Gandhi *et al.*, *Astropart. Phys.* **5** (1996) 81.
13) G.Feldman and R.Cousins, *Phys. Rev.* **D57** (1998) 3873.
14) W.Rhode *et al.*, *Astropart. Phys.* **4** (1994) 217.
15) L.Volkova, *Yad.Fiz.* **31** (1980) 1510 (*Sov. J. Nucl. Phys.* **31** (1980) 784).
16) M.Thunman, G.Ingelman and P.Gondolo, *Astropart. Phys.* **5** (1996) 309.
17) P.Sreekumar *et al.* (EGRET Collaboration), *Ap. J.* **494** (1998) 523.
18) F.W.Stecker and M.H.Salamon, *Astro-ph/9501064.*
19) R.Protheroe, in *Accretion Phenomena and Related Outflows,* Vol. 163 of *IAU Colloquium,* edited by D.Wickramasinghe, G.Bicknell and L.Ferrario (The Astron. Soc. of the Pacific, 1997), pp.585-588, *astro-ph/9809144.*
20) K.Mannheim, R.J.Protheroe and J.P.Rachen, *astro-ph/9812398.*
21) E.Waxman and J.Bahcall, *Phys. Rev.* **D 59** (1999) 023002.
22) K.Mannheim, *astro-ph/0010353.*
23) E.Waxman and J.Bahcall, *Phys. Rev. Lett.* **78** (1997) 2292.
24) P.Bhattacharjee, C.Hill and D.Schramm, *Phys. Rev. Lett.* **69** (1992) 567; G.Sigl, *astro-ph/0008364.*